



LAWRENCE  
LIVERMORE  
NATIONAL  
LABORATORY

# Ab Initio Calculations Of Light-Ion Reactions

P. Navratil, S. Quaglioni, R. Roth, W. Horiuchi

March 13, 2012

Frontier Issues in Physics of Exotic Nuclei (YKIS2011)  
Kyoto, Japan  
October 10, 2011 through October 15, 2011

## **Disclaimer**

---

This document was prepared as an account of work sponsored by an agency of the United States government. Neither the United States government nor Lawrence Livermore National Security, LLC, nor any of their employees makes any warranty, expressed or implied, or assumes any legal liability or responsibility for the accuracy, completeness, or usefulness of any information, apparatus, product, or process disclosed, or represents that its use would not infringe privately owned rights. Reference herein to any specific commercial product, process, or service by trade name, trademark, manufacturer, or otherwise does not necessarily constitute or imply its endorsement, recommendation, or favoring by the United States government or Lawrence Livermore National Security, LLC. The views and opinions of authors expressed herein do not necessarily state or reflect those of the United States government or Lawrence Livermore National Security, LLC, and shall not be used for advertising or product endorsement purposes.

## *Ab initio* calculations of light-ion reactions

Petr NAVRÁTIL<sup>1,2</sup>, Sofia QUAGLIONI<sup>2</sup>, Robert ROTH<sup>3</sup>, and Wataru HORIUCHI<sup>4</sup>

<sup>1</sup>*TRIUMF, 4004 Wesbrook Mall, Vancouver, BC V6T 2A3, Canada*

<sup>2</sup>*Lawrence Livermore National Laboratory, P.O. Box 808, L-414, Livermore, CA 94551, USA*

<sup>3</sup>*Institut für Kernphysik, Technische Universität Darmstadt, 64289 Darmstadt, Germany*

<sup>4</sup>*RIKEN Nishina Center, Wako 351-0198, Japan*

The exact treatment of nuclei starting from the constituent nucleons and the fundamental interactions among them has been a long-standing goal in nuclear physics. In addition to the complex nature of nuclear forces, one faces the quantum-mechanical many-nucleon problem governed by an interplay between bound and continuum states. In recent years, significant progress has been made in *ab initio* nuclear structure and reaction calculations based on input from QCD employing Hamiltonians constructed within chiral effective field theory. In this contribution, we present one of such promising techniques capable of describing simultaneously both bound and scattering states in light nuclei. By combining the resonating-group method (RGM) with the *ab initio* no-core shell model (NCSM), we complement a microscopic cluster approach with the use of realistic interactions and a microscopic and consistent description of the clusters. We discuss applications to light nuclei scattering, radiative capture and fusion reactions.

### §1. Introduction

Nuclei are quantum many-body systems with both bound and unbound states. One of the major challenges for theoretical nuclear physics is to provide a unified description of structural and reaction properties of nuclei that is based on the fundamental underlying physics: the constituent nucleons and the QCD-based realistic interactions among them. A predictive theory of reactions of light nuclei is needed for many reasons.

First, it would greatly help our understanding of nuclear reactions important for astrophysics. Some of the outstanding light-nucleus uncertainty sources in astrophysics applications include: reactions leading to the nucleosynthesis of  $^8\text{B}$  (and the production of the solar neutrinos measured in terrestrial experiments) such as the  $^7\text{Be}(p, \gamma)^8\text{B}$  and  $^3\text{He}(\alpha, \gamma)^7\text{Be}$  radiative capture rates; the thermonuclear reaction rates of  $\alpha$  capture on  $^8\text{Be}$  and  $^{12}\text{C}$  nuclei during the stellar helium burning; and fusion reactions that affect the predictions of Big Bang nucleosynthesis for the abundances of light elements, such as the  $^3\text{He}(d, p)^4\text{He}$ .

Furthermore, nuclear reactions are one of the best tools for studying exotic nuclei, which have become the focus of the next generation experiments with rare-isotope beams. These are nuclei for which most low-lying states are unbound, so that a rigorous analysis requires scattering boundary conditions. In addition, much of the information we have on the structure of these short-lived systems is inferred from reactions with other nuclei.

Finally, low-energy fusion reactions represent the primary energy-generation mechanism in stars, and could potentially be used for future energy generation on earth. Examples of these latter reactions include the  $d+{}^3\text{H}\rightarrow n+{}^4\text{He}$  fusion used at ITER<sup>1)</sup> and at the National Ignition Facility (NIF).<sup>2)</sup> Even though there have been many experimental investigations of the cross sections of this reaction, there are still open issues. A first-principles theory based on accurate two-nucleon ( $NN$ ) and three-nucleon ( $NNN$ ) forces will provide the predictive power to reduce the uncertainty in the reaction rate at very low temperatures; provide an understanding of the reaction rate dependence on the polarization induced by the strong magnetic fields (characteristic of both inertial and magnetic confinement); and clarify the influence of non-local thermal equilibrium in plasma environments.

In this contribution, we describe the recently introduced *ab initio* many-body approach to reactions on light nuclei<sup>3)</sup> that combines the resonating-group method (RGM)<sup>4)</sup> with the *ab initio* no-core shell model (NCSM).<sup>5)</sup> In Sec. 2, we briefly present the NCSM/RGM formalism. In Sect. 3, we discuss examples of calculations relevant for nuclear astrophysics,  ${}^7\text{Be}(p,\gamma){}^8\text{B}$  radiative capture and calculations of the  $d-{}^3\text{He}$  and  $d-{}^3\text{H}$  fusion reactions relevant for energy generation. We also present preliminary results of our  ${}^3\text{He}-{}^4\text{He}$  scattering calculations. Conclusions are given in Sect. 4.

## §2. *Ab initio* NCSM/RGM

The *ab initio* nuclear reaction approach that we are developing is an extension of the *ab initio* no-core shell model (NCSM).<sup>5)</sup> The innovation which allows us to go beyond bound states and treat reactions is the use of cluster basis states in the spirit of the resonating-group method,

$$|\Phi_{\nu r}^{J\pi T}\rangle = \left[ (|A-a \alpha_1 I_1^{\pi_1} T_1\rangle |a \alpha_2 I_2^{\pi_2} T_2\rangle)^{(sT)} Y_\ell(\hat{r}_{A-a,a}) \right]^{(J\pi T)} \frac{\delta(r - r_{A-a,a})}{r r_{A-a,a}}, \quad (2.1)$$

in which each nucleon cluster is described within the NCSM. The above translational invariant cluster basis states describe two nuclei (a target and a projectile composed of  $A - a$  and  $a$  nucleons, respectively) whose centers of mass are separated by the relative coordinate  $\vec{r}_{A-a,a}$  and that are traveling in a  ${}^{2s}\ell_J$  wave or relative motion (with  $s$  the channel spin,  $\ell$  the relative momentum, and  $J$  the total angular momentum of the system). Additional quantum numbers characterizing the basis states are parity  $\pi = \pi_1\pi_2(-1)^\ell$  and total isospin  $T$ . For the intrinsic (antisymmetric) wave functions of the two nuclei we employ the eigenstates  $|A-a \alpha_1 I_1^{\pi_1} T_1\rangle$  and  $|a \alpha_2 I_2^{\pi_2} T_2\rangle$  of the  $(A - a)$ - and  $a$ -nucleon intrinsic Hamiltonians, respectively, as obtained within the NCSM approach. These are characterized by the spin-parity, isospin and energy labels  $I_i^{\pi_i}$ ,  $T_i$ , and  $\alpha_i$ , respectively, where  $i = 1, 2$ . In our notation, all these quantum numbers are grouped into a cumulative index  $\nu = \{A-a \alpha_1 I_1^{\pi_1} T_1; a \alpha_2 I_2^{\pi_2} T_2; s\ell\}$ . Finally, we note that the channel states (2.1) are not antisymmetric with respect to exchanges of nucleons pertaining to different clusters. Therefore, to preserve the Pauli principle one has to introduce the appropriate inter-cluster antisymmetrizer,

schematically

$$\hat{A}_\nu = \sqrt{\frac{(A-a)!a!}{A!}} \left( 1 + \sum_{P \neq id} (-)^p P \right), \quad (2.2)$$

where the sum runs over all possible permutations of nucleons  $P$  different from the identical one that can be carried out between two different clusters (of  $A - a$  and  $a$  nucleons, respectively), and  $p$  is the number of interchanges characterizing them. The operator (2.2) is labeled by the channel index  $\nu$  to signify that its form depends on the mass partition,  $(A - a, a)$ , of the channel state to which is applied.

The channel states (2.1), fully antisymmetrized by the action of the antisymmetrization operator  $\hat{A}_\nu$ , are used as a continuous basis set to expand the many-body wave function,

$$|\Psi^{J^\pi T}\rangle = \sum_\nu \int dr r^2 \hat{A}_\nu |\Phi_{\nu r}^{J^\pi T}\rangle \frac{[\mathcal{N}^{-1/2} \chi]_\nu^{J^\pi T}(r)}{r}, \quad (2.3)$$

where  $\chi_\nu^{J^\pi T}(r)$  represent continuous linear variational amplitudes that are determined by solving the orthogonalized RGM equations:

$$\sum_{\nu'} \int dr' r'^2 [\mathcal{N}^{-\frac{1}{2}} \mathcal{H} \mathcal{N}^{-\frac{1}{2}}]_{\nu\nu'}^{J^\pi T}(r, r') \frac{\chi_{\nu'}^{J^\pi T}(r')}{r'} = E \frac{\chi_\nu^{J^\pi T}(r)}{r}. \quad (2.4)$$

Here  $\mathcal{N}_{\nu\nu'}^{J^\pi T}(r, r')$  and  $\mathcal{H}_{\nu\nu'}^{J^\pi T}(r, r')$ , commonly referred to as integration kernels, are respectively the overlap (or norm) and Hamiltonian matrix elements over the antisymmetrized basis (2.1), *i.e.*:

$$\mathcal{N}_{\nu'\nu}^{J^\pi T}(r', r) = \langle \Phi_{\nu' r'}^{J^\pi T} | \hat{A}_{\nu'} \hat{A}_\nu | \Phi_{\nu r}^{J^\pi T} \rangle, \quad \mathcal{H}_{\nu'\nu}^{J^\pi T}(r', r) = \langle \Phi_{\nu' r'}^{J^\pi T} | \hat{A}_{\nu'} H \hat{A}_\nu | \Phi_{\nu r}^{J^\pi T} \rangle \quad (2.5)$$

where  $H$  is the microscopic  $A$ -nucleon Hamiltonian and  $E$  is the total energy in the center of mass (c.m.) frame. The calculation of the above many-body matrix elements, which contain all the nuclear structure and antisymmetrization properties of the system under consideration, represents the main task in performing RGM calculations. Details on how the integration kernels are calculated and the NCSM/RGM equations solved are given in Refs.<sup>6),7)</sup> In the applications presented in Sec. 3 we employ SRG-evolved<sup>8),9)</sup> chiral N<sup>3</sup>LO<sup>10)</sup>  $NN$  potentials (SRG-N<sup>3</sup>LO).

### §3. Applications

#### 3.1. The ${}^7\text{Be}(p, \gamma){}^8\text{B}$ radiative capture

The  ${}^7\text{Be}(p, \gamma){}^8\text{B}$  radiative capture is the final step in the nucleosynthetic chain leading to  ${}^8\text{B}$  and one of the main inputs of the standard model of solar neutrinos. Recently, we have performed the first *ab initio* many-body calculation,<sup>11)</sup> of this reaction starting from the SRG-N<sup>3</sup>LO  $NN$  interaction with  $\Lambda = 1.86 \text{ fm}^{-1}$ . Using  $p$ - ${}^7\text{Be}$  channel states including the five lowest  $N_{\text{max}} = 10$  eigenstates of  ${}^7\text{Be}$  (the  $\frac{3}{2}^-$  ground and the  $\frac{1}{2}^-$ ,  $\frac{7}{2}^-$ , and first and second  $\frac{5}{2}^-$  excited states), we solved Eq. (2.4)

first with bound-state boundary conditions to find the bound state of  ${}^8\text{B}$ , and then with scattering boundary conditions to find the  $p$ - ${}^7\text{Be}$  scattering wave functions. Former and latter wave functions were later used to calculate the capture cross section, which, at solar energies, is dominated by non-resonant  $E1$  transitions from  $p$ - ${}^7\text{Be}$   $S$ - and  $D$ -waves into the weakly-bound ground state of  ${}^8\text{B}$ . All stages of the calculation were based on the same harmonic oscillator (HO) frequency of  $\hbar\Omega = 18$  MeV, which minimizes the g.s. energy of  ${}^7\text{Be}$ . The largest model space achievable for the present calculation within the full NCSM basis is  $N_{\text{max}} = 10$ . At this basis size, the  ${}^7\text{Be}$  g.s. energy is very close to convergence as indicated by a fairly flat frequency dependence in the range  $16 \leq \hbar\Omega \leq 20$  MeV, and the vicinity to the  $N_{\text{max}} = 12$  result obtained within the importance-truncated NCSM.<sup>12),13)</sup> The choice of  $\Lambda = 1.86 \text{ fm}^{-1}$  in the SRG evolution of the  $\text{N}^3\text{LO}$   $NN$  interaction leads to a single  $2^+$  bound state for  ${}^8\text{B}$  with a separation energy of 136 keV quite close to the observed one (137 keV). This is very important for the description of the low-energy behavior of the  ${}^7\text{Be}(p,\gamma){}^8\text{B}$  astrophysical S-factor, known as  $S_{17}$ . We note that the  $NNN$  interaction induced by the SRG evolution of the  $NN$  potential is repulsive in the  $\Lambda$ -range  $\sim 1.8$ - $2.1 \text{ fm}^{-1}$ , and, in very light nuclei, its contributions are canceled to a good extent by those of the initial attractive chiral  $NNN$  force (which is also SRG evolved).<sup>14),15)</sup>

The resulting  $S_{17}$  astrophysical factor is compared to several experimental data sets in Figure 1. Energy dependence and absolute magnitude follow closely the trend of the indirect Coulomb breakup measurements of Shümann *et al.*,<sup>16),17)</sup> while somewhat underestimating the direct data of Junghans *et al.*<sup>18)</sup> The resonance, particularly evident in these and Filippone's data, is due to the  $M1$  capture, which does not contribute to a theoretical calculation outside of the narrow  ${}^8\text{B}$   $1^+$  resonance and is negligible at astrophysical energies.<sup>19),20)</sup> The  $M1$  operator, for which any dependence upon two-body currents needs to be included explicitly, poses more uncertainties than the Siegert's  $E1$  operator. We plan to calculate its contribution in the future. The shape is also quite similar to that obtained within the microscopic

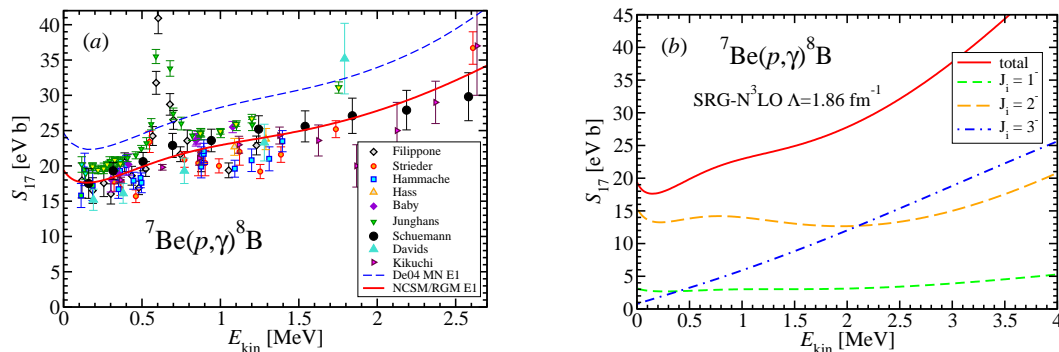


Fig. 1. Calculated  ${}^7\text{Be}(p,\gamma){}^8\text{B}$  S-factor as function of the energy in the c.m. compared to data and the microscopic cluster-model calculations of Ref.<sup>21)</sup> with the Minnesota (MN) interaction (a). Only  $E1$  transitions were considered. Initial-state partial wave contributions are shown in panel (b). Calculation as described in the text.

three-cluster model<sup>21)</sup> (see the dashed line in Fig. 1 (a)) used, after scaling to the data, in the most recent  $S_{17}$  evaluation.<sup>20)</sup> The contributions from the initial  $1^-$ ,  $2^-$  and  $3^-$  partial waves are shown in panel (b) of Fig. 1.

The convergence of our results with respect to the size of the HO model space was assessed by means of calculations up to  $N_{\max} = 12$  within the importance-truncation NCSM scheme<sup>12),13)</sup> with (due to computational limitations) only the first three eigenstates of  ${}^7\text{Be}$ . The  $N_{\max} = 10$  and 12 S-factors are very close. As for the convergence in the number of  ${}^7\text{Be}$  states, we explored it by means of calculations including up to 8  ${}^7\text{Be}$  eigenstates in a  $N_{\max} = 8$  basis (larger  $N_{\max}$  values are currently out of reach with more than five  ${}^7\text{Be}$  states). Based on this analysis, we conclude that the use of an  $N_{\max} = 10$  HO model space is justified and the limitation to five  ${}^7\text{Be}$  eigenstates is quite reasonable. Finally, our calculated  $S_{17}(0) = 19.4(7)$  MeV b is on the lower side, but consistent with the latest evaluation  $20.8 \pm 0.7(\text{expt}) \pm 1.4(\text{theory})$ .<sup>20)</sup>

### 3.2. The ${}^3\text{H}(d, n){}^4\text{He}$ and ${}^3\text{He}(d, p){}^4\text{He}$ fusion reactions

The  ${}^3\text{H}(d, n){}^4\text{He}$  and  ${}^3\text{He}(d, p){}^4\text{He}$  fusion reactions have important implications first and foremost for fusion energy generation, but also for nuclear astrophysics, and atomic physics. Indeed, the deuterium-tritium fusion is the easiest reaction to achieve on earth and is pursued by research facilities directed at reaching fusion power by either inertial (*e.g.*, NIF) or magnetic (*e.g.*, ITER) confinement. Both  ${}^3\text{H}(d, n){}^4\text{He}$  and  ${}^3\text{He}(d, p){}^4\text{He}$  affect the predictions of Big Bang nucleosynthesis for light-nucleus abundances. In addition, the deuterium- ${}^3\text{He}$  fusion is also an object of interest for atomic physics, due to the substantial electron-screening effects presented by this reaction.

In the following we present the first *ab initio* many-body calculations<sup>22)</sup> of these reactions starting from the SRG- $N^3\text{LO}$   $NN$  interaction with  $\Lambda = 1.5 \text{ fm}^{-1}$ , for which we reproduce the experimental  $Q$ -value of both reactions within 1%. We adopted

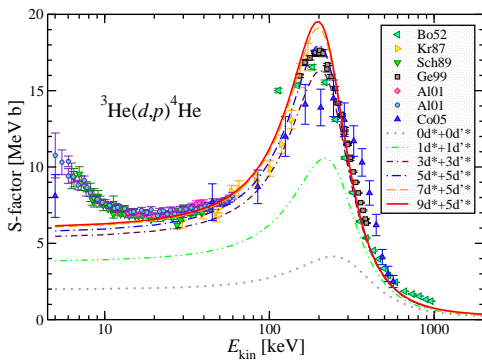


Fig. 2. Calculated S-factor of the  ${}^3\text{He}(d, p){}^4\text{He}$  reaction compared to experimental data. Convergence with the number of deuteron pseudostates in the  ${}^3S_1$ - ${}^3D_1$  ( $d^*$ ) and  ${}^3D_2$  ( $d^{*}$ ) channels.

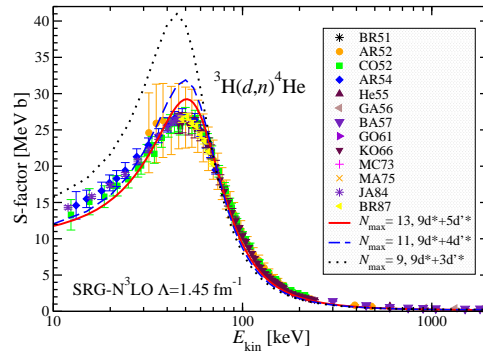


Fig. 3. Calculated  ${}^3\text{H}(d, n){}^4\text{He}$  S-factor compared to experimental data. Convergence with  $N_{\max}$  obtained for the SRG- $N^3\text{LO}$   $NN$  potential with  $\Lambda = 1.45 \text{ fm}^{-1}$  at  $\hbar\Omega = 14 \text{ MeV}$ .

HO model spaces up to  $N_{\max} = 13$  with a frequency of  $\hbar\Omega = 14$  MeV. The channel basis includes  $n$ - $^4\text{He}$  ( $p$ - $^4\text{He}$ ),  $d$ - $^3\text{H}$  ( $d$ - $^3\text{He}$ ),  $d^*$ - $^3\text{H}$  ( $d^*$ - $^3\text{He}$ ) and  $d'^*$ - $^3\text{H}$  ( $d'^*$ - $^3\text{He}$ ) binary cluster states, where  $d^*$  and  $d'^*$  denote  $^3S_1$ - $^3D_1$  and  $^3D_2$  deuterium excited pseudostates, respectively, and the  $^3\text{H}$  ( $^3\text{He}$ ) and  $^4\text{He}$  nuclei are in their ground state.

Figure 2 presents the results obtained for the  $^3\text{He}(d,p)^4\text{He}$  S-factor. The deuteron deformation and its virtual breakup, approximated by means of  $d$  pseudostates, play a crucial role. The S-factor increases dramatically with the number of pseudostates until convergence is reached for  $9d^* + 5d'^*$ . The dependence upon the HO basis size is illustrated by the  $^3\text{H}(d,n)^4\text{He}$  results of Fig. 3. The convergence is satisfactory and we expect that an  $N_{\max} = 15$  calculation, which is currently out of reach, would not yield significantly different results. The experimental position of the  $^3\text{He}(d,p)^4\text{He}$  S-factor is reproduced within few tens of keV. Correspondingly, we find an overall fair agreement with experiment for this reaction, if we exclude the region at very low energy, where the accelerator data are enhanced by laboratory electron screening. The  $^3\text{H}(d,n)^4\text{He}$  S-factor is not described as well with  $\Lambda = 1.5$  fm $^{-1}$ . Due to the very low activation energy of this reaction, the S-factor (particularly peak position and height) is extremely sensitive to higher-order effects in the nuclear interaction, such as three-nucleon force (not yet included in the calculation) and missing isospin-breaking effects in the integration kernels (which are obtained in the isospin formalism). To compensate for these missing higher-order effects in the interaction and reproduce the position of the  $^3\text{H}(d,n)^4\text{He}$  S-factor, we performed additional calculations using lower  $\Lambda$  values. This led to the theoretical S-factor of Fig. 3 (obtained for  $\Lambda = 1.45$  fm $^{-1}$ ), that is in overall better agreement with data, although it presents a slightly narrower and somewhat overestimated peak. This calculation would suggest that some electron-screening enhancement could also be present in the  $^3\text{H}(d,n)^4\text{He}$  measured S factor below 10 keV c.m. energy. However, these results cannot be considered conclusive until more accurate calculations using a complete nuclear interaction (that includes the three-nucleon force) are performed. Work in this direction is under way.

### 3.3. The $^3\text{He}$ - $^4\text{He}$ scattering

Recently, we have extended the NCSM/RGM formalism from the single-nucleon and two-nucleon (deuteron) projectile to the three-nucleon projectile, i.e.,  $^3\text{H}$  and  $^3\text{He}$ . Calculations of  $^3\text{He}$ - $^4\text{He}$  and  $^3\text{H}$ - $^4\text{He}$  are now under way with the ultimate goal to study the  $^3\text{He}(\alpha,\gamma)^7\text{Be}$  and  $^3\text{H}(\alpha,\gamma)^7\text{Li}$  radiative capture. In Fig. 4, we present our preliminary  $^3\text{He}$ - $^4\text{He}$  phase shift results using two SRG-N $^3\text{LO}$   $NN$  potential that we employed in the  $^7\text{Be}(p,\gamma)^8$  and  $^3\text{He}(d,p)^4\text{He}$  calculations discussed in the previous subsections. The virtual breakup of  $^3\text{He}$  ( $^3\text{H}$ ) plays an important role. We take it into account via excited pseudostates of the  $A = 3$  projectile. The shown calculations, performed with the  $N_{\max} = 13$  HO basis expansion, included four pseudostates in the  $1/2^+$  channel. Pseudostates in other channels may be also important, however. Presented results required runs with up to 64,000 cores on the Oak Ridge National Laboratory (ORNL) Jaguar<sup>23)</sup> supercomputer. The softer  $NN$  potential provides more binding of the  $3/2^-$  and  $1/2^-$  bound states and places the  $7/2^-$  and  $5/2^-$  resonances to a lower energy, closer to experiment ( $\sim 2.98$  MeV and

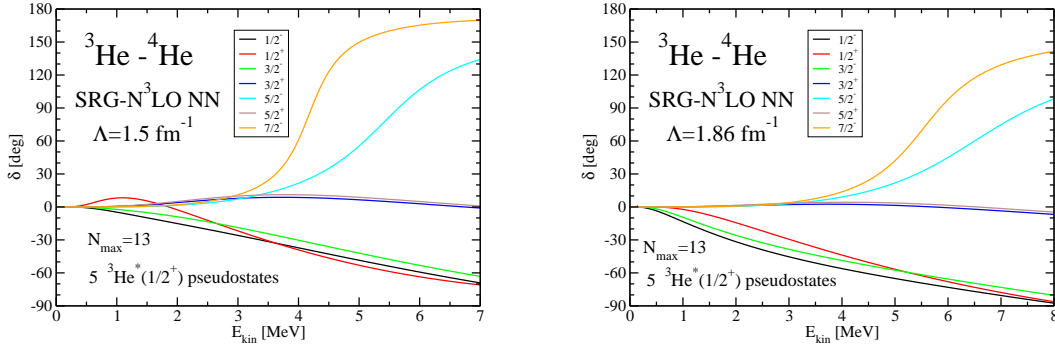


Fig. 4. Preliminary results for the  ${}^3\text{He}$ - ${}^4\text{He}$  scattering phase shifts. The NCSM/RGM calculations, including the g.s. and first four  $1/2^+$  pseudostates of  ${}^3\text{He}$ , were obtained using the SRG- $N^3\text{LO}$   $NN$  potential with  $\Lambda = 1.5 \text{ fm}^{-1}$  (left panel) and  $\Lambda = 1.86 \text{ fm}^{-1}$  (right panel). The HO frequency  $\hbar\Omega = 14 \text{ MeV}$  (left panel) and  $\hbar\Omega = 18 \text{ MeV}$  (right panel) and  $N_{\text{max}} = 13$  basis space were employed.

$\sim 5.14 \text{ MeV}$ , respectively). At the same time, the  $S$ -wave phase shift demonstrates an unexpected behavior becoming positive at low energies. Calculations that include virtual excitations of the  $A = 3$  projectiles in additional channels are now under way. Eventually, we will utilize the bound and scattering wave functions obtained in these calculations to calculate  ${}^3\text{He}(\alpha, \gamma){}^7\text{Be}$  and  ${}^3\text{H}(\alpha, \gamma){}^7\text{Li}$  radiative capture cross sections that are of astrophysical interest.

#### §4. Conclusions and Outlook

We gave an overview of the NCSM/RGM, an *ab initio* many-body approach capable of providing a unified description of structural and reaction properties of light nuclei, by combining the RGM with the use of realistic interactions, and a microscopic and consistent description of the nucleon clusters, achieved via the *ab initio* NCSM. Since the publication of the first results,<sup>3), 6), 24)</sup> obtained for nucleon-nucleus collisions, the NCSM/RGM has grown into a powerful approach for the description of light-ion fusion reactions. The formalism has been extended to include two-nucleon (deuteron) projectiles,<sup>7)</sup> as well as complex reactions with both nucleon-nucleus and deuteron-nucleus channels,<sup>22)</sup> based on realistic  $NN$  interactions. The treatment of three-nucleon ( ${}^3\text{H}$  and  ${}^3\text{He}$ ) projectiles has also been included in the formalism. Further extensions of the approach to include the three-nucleon components of the nuclear interaction and three-cluster channel states are under way.

To apply the present formalism to heavier target nuclei, i.e. heavy  $p$ -shell nuclei and beyond, it becomes necessary to utilize the recently developed importance-truncated NCSM.<sup>12), 13)</sup> This gives us the ability to use large  $N_{\text{max}}$  model spaces, that in the NCSM/RGM approach are of vital importance not just for the convergence of the target and projectile eigenstates but also for the convergence of the localized parts of the integration kernels.<sup>24)</sup>

We are also working on a unification of the original NCSM with the NCSM/RGM

approach presented here. This can be accomplished by coupling the NCSM/RGM basis, consisting of binary-cluster channels with just a few lowest excited states of projectile and target, with the NCSM eigenstates of the composite system as outlined in Ref.<sup>25)</sup> An implementation of this unified approach that we call the no-core shell model with the continuum (NCSMC) is at an advanced stage with promising preliminary results.

### Acknowledgements

Computing support for this work came from the LLNL institutional Computing Grand Challenge program, the Jülich supercomputer Centre and Oak Ridge Leadership Computing Facility at ORNL.<sup>23)</sup> Prepared in part by LLNL under Contract DE-AC52-07NA27344. Support from the U. S. DOE/SC/NP (Work Proposal No. SCW1158), LLNL LDRD grant PLS-09-ERD-020, U. S. DOE/SC/NP (Work Proposal No. SCW0498), the NSERC Grant No. 401945-2011, and from the U. S. Department of Energy Grant DE-FC02-07ER41457 is acknowledged. This work is supported in part by the Deutsche Forschungsgemeinschaft through contract SFB 634 and by the Helmholtz International Center for FAIR within the framework of the LOEWE program launched by the State of Hesse. W.H. was supported by the Special Postdoctoral Researchers Program of RIKEN.

### References

- 1) ITER URL <http://www.iter.org>
- 2) NIF URL <https://lasers.llnl.gov>
- 3) S. Quaglioni and P. Navrátil, *Phys. Rev. Lett.* **101** (2008), 092501
- 4) K. Wildermuth and Y. C. Tang, *A unified theory of the nucleus* (Vieweg, Braunschweig) (1977)
- 5) P. Navrátil, J. P. Vary, and B. R. Barrett, *Phys. Rev. Lett.* **84** (2000), 5728
- 6) S. Quaglioni and P. Navrátil, *Phys. Rev. C* **79** (2009), 044606
- 7) P. Navrátil and S. Quaglioni, *Phys. Rev. C* **83** (2011), 044609
- 8) S. K. Bogner, R. J. Furnstahl, and R. J. Perry, *Phys. Rev. C* **75** (2007), 061001
- 9) R. Roth, S. Reinhardt and H. Hergert, *Phys. Rev. C* **77** (2008), 064003
- 10) D. R. Entem and R. Machleidt, *Phys. Rev. C* **68** (2003), 041001
- 11) P. Navrátil, R. Roth, and S. Quaglioni *Physics Letters B* **704** (2011), 379 – 383
- 12) R. Roth and P. Navrátil, *Phys. Rev. Lett.* **99** (2007), 092501
- 13) R. Roth, *Phys. Rev. C* **79**, (2009) 064324
- 14) E. D. Jurgenson, P. Navrátil, and R. J. Furnstahl, *Phys. Rev. Lett.* **103** (2009), 082501
- 15) E. D. Jurgenson, P. Navrátil, and R. J. Furnstahl, *Phys. Rev. C* **83** (2011), 034301
- 16) F. Schümann *et al.*, *Phys. Rev. Lett.* **73** (2003 ), 232501
- 17) F. Schümann *et al.*, *Phys. Rev. C* **73** (2006 ), 015806
- 18) A. R. Junghans *et al.*, *Phys. Rev. C* **68** (2003), 065803
- 19) E. Adelberger *et al.*, *Rev. Mod. Phys.* **83** (2011), 195
- 20) E. Adelberger *et al.*, *Rev. Mod. Phys.* **70** (1998 ), 1265
- 21) P. Descouvemont, *Phys. Rev. C* **70** (2004), 065802
- 22) P. Navrátil and S. Quaglioni, *Phys. Rev. Lett.* **108** (2012), 042503
- 23) Information on Jaguar can be found at the URL <http://www.nccs.gov>
- 24) P. Navrátil, R. Roth and S. Quaglioni, *Phys. Rev. C* **82** (2010), 034609
- 25) P. Navratil, S. Quaglioni, I. Stetcu and B. R. Barrett, *J. Phys. G: Nucl. Part. Phys.* **36** (2009), 083101